curve LM to merger of the nonsymmetric modes and their disappearance. The dashed line corresponds to an approximate condition for disturbance of the symmetry ($\varkappa_* = 4e$) according to (2.2) and (2.3).

It is interesting that the instability domain of the symmetric mode NLK corresponds to the bistability domain obtained in [2].

Taking account of the results obtained for the flow considered, it can be assumed that a thermal instability can result in flow partition into a jet in the filtration of a strongly viscous fluid in a mode with determination of the total flow rate. Thermal wave propagation across the filtering stream is possible in case of head determination.

The authors are grateful to A. G. Merzhanov for interest in the research.

LITERATURE CITED

1. S. A. Bostandzhiyan, A. G. Merzhanov, and S. I. Khuyaev, "On a hydrodynamic thermal explosion," Dokl. Akad. Nauk SSSR, 163, No. 1 (1965).
2. A. G. Merzhanov and A. M. Stolin, "Hydrodynamic analogs of the ignition and extinction phenomena," Zh. Prikl. Mekh. Tekh. Fiz., No. 1 (1974).
3. A. F. Volkov and Sh. M. Kogan, "Physical phenomena in semiconductors with negative differential conductivity," Usp. Fiz. Nauk, 96, No. 4 (1968).
4. V. V. Grachev and É. N. Rumanov, "Thermal breakdown suppression modes," Dokl. Akad. Nauk SSSR, 263, No. 3 (1982).
5. D. A. Frank-Kamenetskii, Diffusion and Heat Transfer in Chemical Kinetics [in Russian], Nauka, Moscow (1967).

MIXED LAMINAR CONVECTION AROUND A VERTICAL CYLINDER WITH A CONSTANT SURFACE TEMPERATURE

Yu. P. Semenov

UDC 536.244

The heat exchange accompanying mixed convection around vertical cylinders plays an important role in many technological processes and in the operation of power plants. However, this problem has not been studied to a sufficient extent. Most papers concerned with mixed laminar convection are devoted to processes on vertical flat surfaces [1, 2] and horizontal cylinders [3]. The heat exchange due to mixed convection from vertical cylinders has been investigated in individual papers only. The problem of concurrent mixed convection from a vertical cylinder with a constant surface temperature is solved in [4] by means of the method of local non-self-similarity, which is also used in [5] for solving this problem for a constant thermal flux q_w. Mixed convection from a vertical cylinder for q_w = const was investigated experimentally and numerically in [6, 7]. Thus, mixed laminar convection from vertical cylinders for t_w = const has been investigated only in [4]. However, the mixed convection parameter varied there in the limited range $0 \leqslant Gr/Re^2 \leqslant 2$; generalized theoretical relationships were not derived, and only concurrent convection was contemplated. This made it necessary to undertake the investigation described here.

Mixed convection from vertical cylinders constitutes a non-self-similar problem. The method of local non-self-similarity used in [4, 5] is approximate. In order to obtain the solution for the entire region of mixed convection, it is necessary to solve the boundary layer equations written in terms of self-similar variables of forced motion in a region close to the forced motion and the boundary layer equations written in terms of self-similar variables of natural convection in a region close to the natural convection. In this case, it is more advisable to obtain directly the numerical solution of the boundary layer equations.

The method described in [8, 9] is used for solving numerically the problem of mixed convection from a vertical cylinder. This method was used in [7] for investigating mixed convection from a vertical cylinder for q_w = const and in [10] for investigating natural convection.

Moscow. Translated from Zhurnal Prikladnoi Mekhaniki i Tekhnicheskoi Fiziki, No. 1, pp. 47-52, January-February, 1984. Original article submitted November 1, 1982.

 0021-8944/84/2501-0042$08.50

The initial system of equations in a cylindrical coordinate system is written in the following form:

the equation of motion,

$$\rho u \frac{\partial u}{\partial x} + \rho v \frac{\partial u}{\partial y} = \frac{1}{r}\frac{\partial}{\partial y}\left(r\mu \frac{\partial u}{\partial y}\right) - \frac{dp}{dx} \pm \rho g; \tag{1}$$

the energy equation,

$$\rho u \frac{\partial i}{\partial x} + \rho v \frac{\partial i}{\partial y} = \frac{1}{r}\frac{\partial}{\partial y}\left(r\lambda \frac{\partial i}{\partial y}\right); \tag{2}$$

the continuity equation,

$$\partial(\rho r u)/\partial x + \partial(\rho r v)/\partial y = 0, \tag{3}$$

where x and y are the longitudinal and the radial coordinates (the y coordinate is measured from the cylinder surface); $r = R + y$ (R is the cylinder radius), u and v are the longitudinal and the radial velocity components, i is the enthalpy, p is the pressure, ρ is the density, μ is the dynamic viscosity coefficient, λ is the thermal conductivity coefficient, and g is the acceleration due to gravity.

The plus sign in front of the term ρg in Eq. (1) corresponds to concurrent mixed convection, while the minus sign corresponds to nonconcurrent convection.

We introduce a new variable instead of y,

$$\omega = (\psi - \psi_w)/(\psi - \psi_0), \tag{4}$$

where ψ is the stream function, defined by the relationships

$$\partial\psi/\partial y = \rho u r,\ \partial\psi/\partial x = -\rho v r; \tag{5}$$

ψ_w and ψ_0 are the stream function values at the wall and at the outer boundary of the boundary layer, respectively.

In our case, $\partial\psi_w/\partial x = 0$, $\partial\psi_0/\partial x = -r_0 m_0$, where r_0 is the radius and m_0 is the mass flow at the outer boundary of the boundary layer.

For $du_0/dx = 0$, considering (4) and (5), we write the initial system (1)-(3) in the following form in an x versus ω coordinate system:

$$\frac{\partial u}{\partial x} + \frac{\omega r_0 m_0}{\psi_0 - \psi_w}\frac{\partial u}{\partial \omega} = \frac{\partial}{\partial \omega}\left[\frac{r^2 \rho\mu u}{(\psi_0 - \psi_w)^2}\frac{\partial u}{\partial \omega}\right] \pm \frac{g(\rho_0 - \rho)}{\rho u}; \tag{6}$$

$$\frac{\partial i}{\partial x} + \frac{\omega r_0 m_0}{\psi_0 - \psi_w}\frac{\partial i}{\partial \omega} = \frac{\partial}{\partial \omega}\left[\frac{r^2 \rho u\lambda}{(\psi_0 - \psi_w)^2}\frac{\partial i}{\partial \omega}\right]. \tag{7}$$

Equations (6) and (7) are integrated numerically. The calculation scheme developed in [8, 9] is utilized fully here. The method of progressive integration is used. Some of the features of the scheme are: The derivatives with respect to ω are determined for the function values at the end of the longitudinal integration interval; the variable changes linearly between the nodal points in the transverse direction; along the longitudinal coordinate, the dependent variables change in steps, and the value of the variable along the entire interval, except at the initial point, is equal to its value at the end of the interval. The assumption of linear variation of the functions with respect to ω may cause an error in determining their values near the wall, which would affect the accuracy of friction and heat-exchange determinations. Therefore, a power distribution of functions is assumed near the wall, while the exponent is determined on the basis of the solution for Couette flow. The difference equations are obtained by expressing each term of the differential equations in the form of the mean-integral value in the control volume.

In order to obtain the solution, it is necessary to assign the initial velocity and enthalpy distributions and the conditions at the wall and the outer boundary. We assume that the velocity and temperature distributions before the first interval are uniform. The conditions at the wall and the outer boundary are assigned in the usual manner. Determination of the physical outer integration boundary and of the physical transverse coordinates involves certain difficulties. The integration domain $0 \leqslant \omega \leqslant 1$ must include all points with real

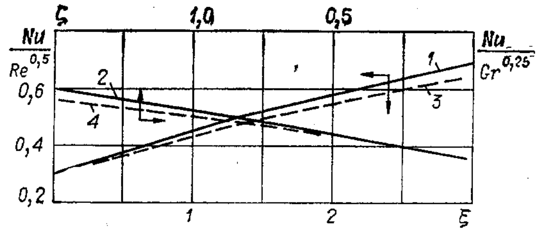

Fig. 1

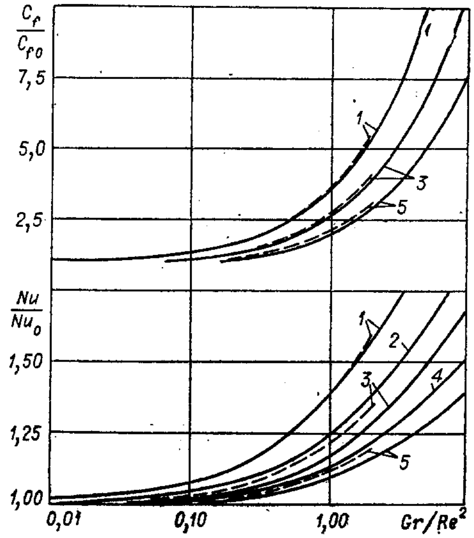

Fig. 2

gradients of the dependent variables. The inner boundary coincides with the wall, while the outer boundary can be determined indirectly in terms of the rate of exchange through the outer boundary of the boundary layer m_0. In order to determine m_0, Eq. (6) is written for ω_* at a certain distance from ω_0 inside the layer:

$$r_0 m_0 = \left\{\frac{\frac{\partial}{\partial\omega}\left[\frac{r^2\rho u\mu}{\psi_0-\psi_w}\frac{\partial u}{\partial\omega}\right]}{\partial u/\partial\omega}\right\}_* - \frac{\psi_0-\psi_w}{(\partial u/\partial\omega)_*}\left[\mp\frac{g(\rho_0-\rho)}{\rho u}\right]_*.$$

Evidently, the value of ω_* must differ slightly from 1. For the conditions under consideration, we can assume that $[g(\rho_0 - \rho)/\rho u]_* \approx 0$, and we then have

$$r_0 m_0 = \left\{\frac{\frac{\partial}{\partial\omega}\left[\frac{r^2\rho u\mu}{\psi_0-\psi_w}\frac{\partial u}{\partial\omega}\right]}{\partial u/\partial\omega}\right\}_*.$$

The derived relationships are used for determining the physical width of the integration domain and the physical coordinates of the calculation grid.

If we have a uniform grid with respect to ω, the chosen x vs ω coordinate system makes it possible to obtain the necessary grid with respect to y. The spacing along x is variable and is related to the boundary layer thickness. The longitudinal spacing is proportional to the square of the layer thickness.

One of the basic features of the method is the procedure for determining the heat flux and friction at the wall. It is assumed that the Couette flow equations can be used for a thin layer at the wall. By solving these equations for a flat wall, we obtain the necessary relationships:

$$\frac{c_f}{2} = \frac{1}{\mathrm{Re}^+} - \frac{y}{2(\rho u)^2}[\mp g(\rho_0-\rho)]; \quad (8)$$

$$\mathrm{St} = 1/(\mathrm{Pr}\,\mathrm{Re}^+), \quad (9)$$

where c_f is the friction coefficient, St is the Stanton number, Pr is the Prandtl number, and $\mathrm{Re}^+ = \rho u y/\mu$.

The effect of axial symmetry is neglected in deriving Eqs. (8) and (9), which may produce a calculation error for a large axial symmetry parameter $\xi = 4(x/R)\mathrm{Re}^{-0.5}$, where $\mathrm{Re} = \rho u_0 x/\mu$.

The numerical solution has been obtained by means of a Minsk-32 computer. The program, based on the FORTRAN language, was composed by using the program from [9] with the necessary modifications. The program adjustment was effected by using the example of heat exchange with forced flow over a plate. The calculation grid was established experimentally. We used

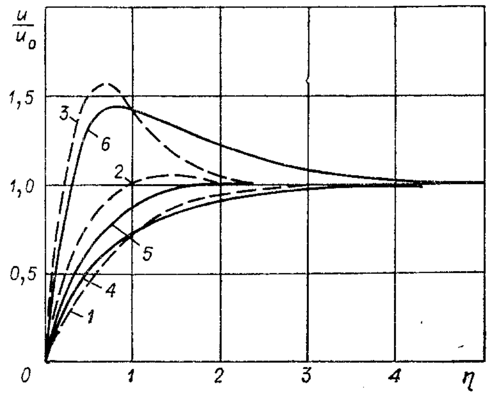

Fig. 3

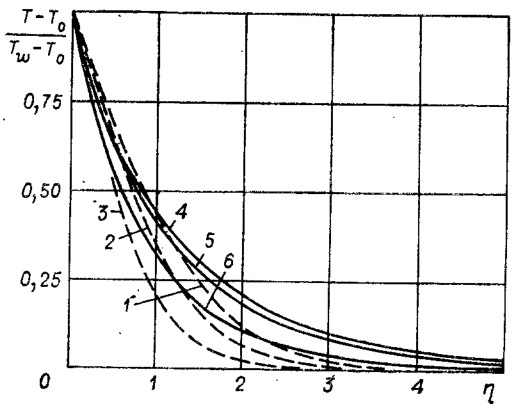

Fig. 4

30 grid nodes in the direction across the layer.

The calculations were performed for Pr = 0.7. Along with forced flow calculations, we performed calculation of mixed convection from a vertical plate for $0 \leqslant Gr/Re^2 \leqslant 10$ [$Gr = g\beta x^3(T_w - T_0)\rho^2/\mu^2$; $Re = \rho u_0 x/\mu$] for the approval of the method. The calculation results are in good agreement with the data from [2, 4]; they are generalized in accordance with the equation

$$Nu^*/Nu_0^* = [1 + 2.19\,(Gr/Re^2)^{3/4}]^{1/3}, \tag{10}$$

where $Nu^*_0 = 0.295\ Re^{0.5}$ is the Nusselt number for forced flow over the plate. In this case and elsewhere, T_0 is used as the determining temperature, while x is the determining dimension. Equation (10) allows the limiting process for passage to forced or natural convection.

The calculation results for forced convection ($Gr/Re^2 < 0.01$) and for conditions close to natural convection ($Gr/Re^2 \approx 10$) are shown in Fig. 1 [curves 1 and 2; $\zeta = 2.83\ (x/R) \times Gr^{-0.25}$]. For comparison, this diagram also shows the data for forced flow [4] (curve 3) and natural convection [11] (curve 4). We observe satisfactory agreement between the results. Within the ranges $\xi \leqslant 3$ and $\zeta \leqslant 1.5$, the discrepancy does not exceed 6%. With a further increase in ξ and ζ, the discrepancy increases, which is, obviously, explained by the use of Eqs. (8) and (9) for calculating St and $c_f/2$.

The results obtained in calculating the heat exchange and friction for concurrent convection are shown in Fig. 2 (the subscript 0 pertains to forced flow parameters). This figure also shows the results obtained in [4] (dashed curves). The data on friction show good correlation with those from [4]. With respect to heat exchange, the results for the plate ($\xi = 0$) are in agreement. The discrepancy increases with ξ, but does not exceed 5% (the values $\xi = 0$; 0.5; 1; 2; 3 pertain to curves 1-5, respectively).

Analysis of Fig. 2 indicates that the effect of buoyancy diminishes with an increase in the parameter ξ. The value of the parameter Gr/Re^2 below which the effect of natural convection is negligible is shifted toward larger values with an increase in ξ. Thus, for $\xi = 3$ and $Gr/Re^2 < 0.4$, the effect of natural convection is not larger than 5%. For a plate, however, this occurs when $Gr/Re^2 < 0.01$.

Natural convection exerts a greater influence on friction than on the heat exchange. It decreases with an increase in ξ.

Figures 3 and 4 show examples of the velocity and temperature profiles for $Gr/Re^2 =$ 0.28; 1.35; 5.69; 0.55; 1.13; 5.16 and $\xi = 0.5$; 0.5; 0.5; 3.03; 3.01; 3 (curves 1-6, respectively).

The results of heat-exchange calculations are approximated with an error of less than 5% by means of the expression

$$Nu = Nu^* + Ax/R,$$

where Nu^*, the Nusselt number for mixed convection from a plate, is determined by means of Eq. (10).

The A coefficient is a function of Gr/Re^2. For determining this coefficient, we have derived the expression

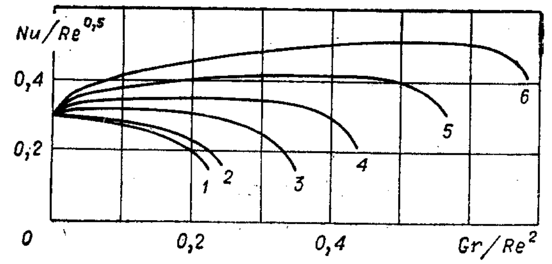

Fig. 5

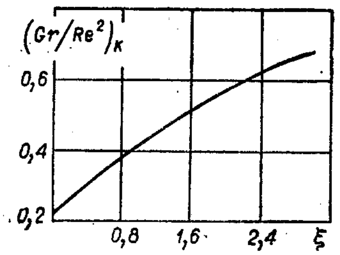

Fig. 6

$$A = 0.53 - 0.032[2 + \lg(\mathrm{Gr}/\mathrm{Re}^2)],$$

which holds for $0.01 \leqslant \mathrm{Gr}/\mathrm{Re}^2 \leqslant 10$. If $\mathrm{Gr}/\mathrm{Re}^2 \leqslant 0.01$, A = 0.53, which corresponds to data for purely forced convection [4], and if $\mathrm{Gr}/\mathrm{Re}^2 \geqslant 10$, A = 0.435, which pertains to purely natural convection [11].

We performed calculations for nonconcurrent mixed convection in the region close to forced motion. Figure 5 shows the calculation results for the flow around cylinders with different diameters, i.e., with $\xi/x^{0.5}$ = 0; 0.53; 2.6; 4.2; 6.2; 8.8 (curves 1-6, respectively). Separation of the boundary layer occurs in the case of nonconcurrent mixed convection. It is evident from Fig. 5 that, with an increase in the parameter of axial symmetry, separation occurs for large values of $\mathrm{Gr}/\mathrm{Re}^2$. It is known that the time of separation cannot be accurately determined within the framework of the boundary layer theory. We can only speak of approximate values of the separation parameters. In our work, the calculations came to an end when zero velocity was obtained at the first calculation node away from the wall, which approximately coincided with a sharp drop in heat transfer. For these conditions, we have derived an expression (Fig. 6) for the ratio $(\mathrm{Gr}/\mathrm{Re}^2)_k$ as a function of the parameter ξ. The dependence is approximated by the equation

$$(\mathrm{Gr}/\mathrm{Re}^2)_k = 0.22 + 0.225\xi - 0.025\xi^2.$$

We did not succeed in deriving a simple expression for calculating the heat exchange in the case of nonconcurrent convection. The diagram of Fig. 5 can be used as a nomogram for approximate calculations of heat transfer.

LITERATURE CITED

1. O. G. Martynenko and Yu. A. Sokovishin, Heat Exchange by Mixed Convection [in Russian], Nauka i Tekhnika, Minsk (1975).
2. P. M. Brdlik, A. I. Il'inskii, and Yu. P. Semenov, "Control of heat and mass exchange in the case of mixed convection in the boundary layer," in: Heat and Mass Exchange — VI [in Russian], Vol. 1, ITMO, Minsk (1980), Part 3.
3. V. A. Belyakov, P. M. Brdlik, and Yu. P. Semenov, "Experimental investigation of mixed air convection around a horizontal cylinder," Zh. Prikl. Mekh. Tekh. Fiz., No. 2 (1980).
4. C. Mokoglu, "Effect of buoyancy on forced convection along a vertical cylinder," Teploperedacha, No. 2 (1975).
5. C. Mokoglu, "Effect of buoyancy on forced convection along a vertical cylinder with a constant thermal flux at the surface," Teploperedacha, No. 3 (1976).
6. P. M. Brdlik, Yu. P. Semenov, et al., "Experimental investigation of mixed convection from vertical surfaces," Scientific Papers, Moscow Forestry Engineering Institute [in Russian], Vol. 138 (1981).
7. Yu. P. Semenov, "Numerical investigation of laminar mixed convection around a vertical cylinder with a constant thermal flux at the surface," Scientific Papers, Moscow Forestry Engineering Institute [in Russian], Vol. 146 (1982).
8. S. V. Patankar and D. B. Spalding, Heat and Mass Transfer in Boundary Layers, 2nd edn., Intext (1971).
9. S. V. Patankar and D. B. Spalding, Heat and Mass Transfer in Boundary Layers, 2nd edn., Intertext Books, London (1971).
10. H. B. Mason and R. A. Seban, "Numerical predictions for turbulent free convection from vertical surfaces," Int. J. Heat Mass Transfer, 17, 1329 (1974).
11. T. Fujii and H. Uehara, "Laminar convective hat transfer from the outer surface of a vertical cylinder," Int. J. Heat Mass Transfer, 13, 607 (1970).